

CHAPTER 5

A SPECTRAL MODEL FOR WAVES IN THE NEAR SHORE ZONE

R. C. Ris¹, L.H. Holthuijsen¹ and N. Booij¹

Abstract

The present paper describes the second phase in the development of a fully spectral wave model for the near shore zone (SWAN). Third-generation formulations of wave generation by wind, dissipation due to whitecapping and quadruplet wave-wave interactions are added to the processes of (refractive) propagation, bottom friction and depth-induced wave breaking that were implemented in the first phase (Holthuijsen et al., 1993). The performance and the behaviour of the SWAN model are shown in two observed cases in which waves are regenerated by the wind after a considerable decrease due to shallow water effects. In the case of the Haringvliet (a closed branch of the Rhine estuary, the Netherlands) reasonable results in terms of significant wave heights were obtained. In the case of Saginaw Bay (Lake Huron, USA), the SWAN model underestimates the significant wave height deep inside the bay (as did two other models). Due to the absence of triad wave-wave interactions in the model the mean period is not properly shifted to the higher frequencies in shallow water. Adding these triads is planned for the next phase of developing the SWAN model.

Introduction

In conventional wave models (at least in coastal engineering) wave components are traced from deep water into shallow water along wave rays to obtain realistic estimates of wave parameters in coastal areas, lakes and estuaries. However, this technique often results in chaotic wave ray patterns which are difficult to interpret. Moreover, nonlinear processes cannot be calculated efficiently. Using a spectral wave model that represents the evolution of the waves on a grid is superior in several respects. The inherent spatial smoothing of such a model ensures a realistic smooth representation of the wave pattern, and it allows an efficient representation of the random, short-crested waves with their generation and dissipation. Models of

¹ Delft University of Technology, Department of Civil Engineering, Stevinweg 1, 2628 CN, Delft, The Netherlands.

this type are fairly common for oceans and shelf seas. However in coastal applications several orders of magnitude more computer effort is required due to the very high spatial resolution that is needed and the numerical techniques that are used. We reduced the required computer effort greatly by considering stationary situations only and by developing an unconditionally stable propagation scheme. The model is described and results are shown of tests for observed conditions in the Haringvliet and in Saginaw Bay with effects of wind, whitecapping, quadruplet wave-wave interactions, bottom friction and depth-induced wave breaking included.

Model formulation

The SWAN model (Simulation of Waves in Near shore areas) is conceived to be a third-generation, stationary wave model that is discrete spectral in both frequencies and directions. The qualification "third-generation" implies that the spectrum in the model evolves free from any a priori restraints (Komen et al., 1994). The model is formulated in terms of action density N (energy density divided by relative frequency: $N = E/\sigma$). From the possible representations of the spectrum in frequency, direction and wave number space, we choose a formulation in terms of relative frequency σ and direction of propagation θ (normal to the wave crest of a wave component). This is convenient for two reasons. Because of efficiency and accuracy, an implicit numerical scheme should be chosen for energy transport across the directions (refraction) and an explicit scheme for energy transport across the frequencies or wave numbers (frequency or wave number shift). The latter is subject to a Courant stability criterion which is more restrictive for the wave number formulation than the formulation in terms of frequency. Choosing the relative frequency σ rather than absolute frequency ω has the advantage that the relationship between the relative frequency and wave number remains unique when currents are added.

In general the evolution of the spectrum can be described by the spectral action balance equation (e.g., Phillips, 1977):

$$\frac{\partial}{\partial t} N(\sigma, \theta) + \nabla_{x,y} \cdot [(c_g + \underline{U}) N(\sigma, \theta)] + \frac{\partial}{\partial \sigma} [c_\sigma N(\sigma, \theta)] + \frac{\partial}{\partial \theta} [c_\theta N(\sigma, \theta)] = \frac{S(\sigma, \theta)}{\sigma} \quad (1)$$

The first term in the left-hand side is the rate of change of action density in time, the second term is the rectilinear propagation of action in geographical x, y -space. The third term describes the shifting of the relative frequency due to currents and unsteadiness of depths with propagation velocity c_σ in σ -space. The fourth term represents the propagation in θ -space (depth and current induced refraction) with propagation velocity c_θ . This action balance equation implicitly takes into account the interaction between waves and currents through radiation stresses. The term $S(\sigma, \theta)$ at the right hand side of the action balance equation is the source term representing the growth by wind, the wave-wave interactions and the decay by bottom friction, whitecapping and depth-induced wave breaking.

To reduce computer time, we removed time from the action balance equation (i.e., $\partial/\partial t = 0$). This is acceptable for most coastal conditions since the residence time of the waves is usually far less than the time scale of variations of the wave boundary condition, the ambient current or the tide. For cases in which the time scale of these variations becomes important, i.e., variable incoming waves at the boundary, or variable winds or currents, a quasi-stationary approach can be taken by repeating the computations for predefined time intervals. For the wind effects the formulations of Cavaleri and Malanotte-Rizzoli (1981) and Snyder et al. (1981) are used. For the bottom friction effects the formulation from JONSWAP (Hasselmann et al., 1973; WAMDI group, 1988) is taken with the friction coefficient Γ equal $0.067 \text{ m}^2\text{s}^{-3}$ (wind sea conditions; Bouws and Komen, 1983). Whitecapping is represented by the formulation of Hasselmann (1974) and Komen et al. (1984) in which the dissipation is controlled primarily by the steepness of the waves. Depth-induced wave breaking is modelled by a spectral version of the Battjes/Janssen wave breaking model (Battjes and Janssen, 1978) resulting in a dissipation which does not affect the shape of the spectrum itself (Beji and Battjes, 1993; Battjes et al., 1993). For the breaking coefficient in this model we use $\gamma=0.73$ which is the average value in the field experiments summarized in Table 1 of Battjes and Stive (1985). The quadruplet wave-wave interactions of Hasselmann (1962) are calculated with the Discrete Interaction Approximation (DIA) of Hasselmann et al. (1985) as in the WAM model (WAMDI group, 1989). A complete version of the SWAN model is planned to include triad wave-wave interactions. In very shallow water these triad wave-wave interactions transfer energy to higher frequencies. However, the triad interactions are still poorly understood and no suitable expression in terms of energy density has yet been derived (only for non-dispersive waves, Abreu et al., 1992). Efforts are presently being made to model the triad interactions based on the work of other authors, e.g., Beji and Battjes (1993), Battjes et al. (1993) and Madsen et al. (1991).

The numerical algorithm

In coastal wave models it is customary to propagate waves from deeper water towards the shore. In the HISWA model (Holthuijsen et al., 1989) this is exploited by propagating the waves line by line roughly parallel with the crests from deeper water to shallower water over a regular grid. This is computationally very efficient and unconditionally stable from a numerical point of view but waves can only propagate within a directional sector of about 120° . Complicated wave conditions with extreme refraction, reflections or initial cross seas cannot be properly accommodated. In the SWAN model we retain the unconditionally stable character of this technique but we expand it to accommodate these complicated conditions (wave from all directions). This modified version of the technique of the HISWA model (which in turn was borrowed from parabolic refraction/diffraction models) is a forward marching scheme in geographic x,y -space in a sequence of four 90° sectors of wave propagation (quadrants). In the first quadrant the state in a gridpoint (x_i, y_j) is determined by its up-wave gridpoints (x_{i-1}, y_j) and (x_i, y_{j-1}) .

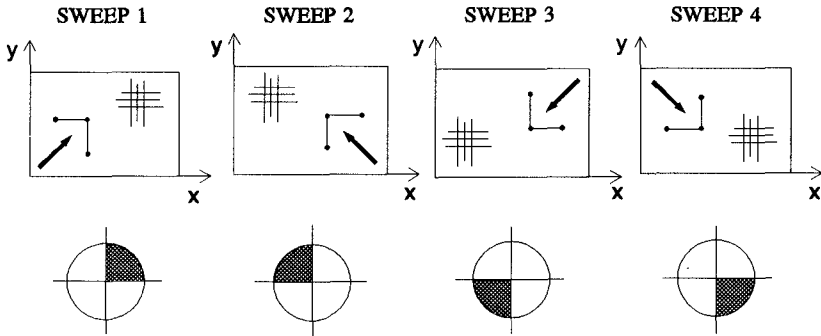


Fig. 1 Numerical scheme for wave propagation in geographic space in SWAN with the appropriate directional quadrant indicated per sweep for which the waves are propagated.

The computation is therefore unconditionally stable for all wave propagation directions in the 90° quadrant between the up-wave x - and y -direction because the wave characteristics lie within this quadrant. The waves in this quadrant are propagated with this scheme over the entire geographical region on a rectangular grid (sweep 1, Fig. 1). By rotating the stencil over 90° , the next quadrant (90° - 180°) is propagated (sweep 2). Rotating the stencil twice more ensures propagation within all four quadrants. This allows waves to propagate from all directions with an unconditionally stable scheme. In cases with current- or depth induced refraction, action density can shift from one quadrant to another. This is taken into account through the boundary conditions of the directional quadrants and by repeating the computations with converging results. Hence the method is characterized as an iterative four-sweep technique (Holthuijsen et al., 1993). Typically we choose a change of less than 1% in significant wave height and mean wave period in 99% of the wetted geographic gridpoints to terminate the iteration. The propagation in θ -direction (refraction) is computed with an implicit scheme to achieve numerical stability for large bottom gradients (central second-order scheme). The corresponding tri-diagonal matrix is solved with a Thomas algorithm (Abbott and Basco, 1989). Preliminary results of propagation tests (also with currents induced wave blocking) for analytical and real cases show an accurate and stable behaviour of the wave model. In all of the next cases, however, no currents are present.

The integration of the source terms is straightforward for all frequencies of the discretized spectrum (the prognostic part of the spectrum, $\sigma < \sigma_{\max}$). For frequencies higher than σ_{\max} , a diagnostic spectral tail is added to the spectrum. To ensure a stable integration of the source terms we have used explicit schemes for the input

source terms and semi-implicit and fully implicit schemes for the sink terms. To suppress the development of numerical instabilities, the maximum growth of energy density per sweep in a spectral bin is limited to a fraction of 10% (Tolman, 1992) of the fully developed equilibrium level (Phillips, 1958). Decay is not similarly limited to allow realistic rapid decrease near the shore. In SWAN the frequency σ is exponential distributed ($\sigma_{i+1} = \alpha\sigma_i$, with α constant) so that the calculation of the nonlinear transfer scales with frequency and can be integrated economically.

Field measurements: the Haringvliet and Saginaw bay

We will concentrate on a comparison with observations in two observed cases in which regeneration after decay is dominant. Both cases are in shallow water with an initial decrease of wave energy due to dissipation and refraction and a subsequent increase of wave energy due to wind. One is taken from the Haringvliet in the Netherlands (a closed branch of the Rhine estuary; Holthuijsen et al. 1989; Holthuijsen et al., 1993). Here a shoal protects the branch (5 km length scale) from the open sea (see Fig. 2). The computations have been carried out for a situation which occurred on October 14, 1982 at 23:00 h (1.95 m depth over the top of the shoal). The waves are locally generated in the southern North Sea and approach the estuary from NW direction and travel across and around the shoal. The observations show that a considerable fraction of wave energy is dissipated over the shoal. Behind the shoal the waves are regenerated by the wind. The wind speed was 16.5 m/s from NW. During this period currents were practically absent. The other case is taken from Saginaw Bay (USA; Bondzie and Panchang, 1993). Here a shallow region with an island protects the bay (25 km length scale) from Lake Huron (see Fig. 3). During a storm event in May, 1981 wave conditions were recorded with wave gauges at three locations (A, B and C). The wind velocity was 11.2 m/s, blowing along the main axis of the bay from Lake Huron. The observed wave height initially decreases between location A and B and then increases between location B and C.

Model results for the Haringvliet

The resolution of the bottom grid for the Haringvliet is $\Delta x = 500$ m and $\Delta y = 500$ m. The directional resolution in the spectrum is $\Delta\theta = 10^\circ$ and the frequency resolution is $\Delta f = 0.1045 \cdot f$ between 0.055 Hz and 0.66 Hz. The observed wave boundary conditions at location 1 (see Fig. 2) are a significant wave height $H_s = 3.54$ m and a peak period $T_p = 8.3$ s. A JONSWAP spectrum is assumed at this up-wave boundary with a $\cos^2(\theta)$ directional distribution since the observed width of the directional energy distribution is about 31° . We carried out two calculations with the SWAN model to show the effects of the regeneration of wave energy by wind: one with and one without wind. Fig. 2 shows the pattern of the significant wave height. The results indicated in Table 1 as "wind" are obtained with all mechanisms of generation and dissipation activated (the same station identification as in Holthuijsen et al. (1989) is used). Note that no measurements are available for location 2 at

23.00 h. The significant wave height thus computed agrees fairly well with the observations. The results indicated in Table 1 as "no wind" are obtained with only depth-induced breaking and bottom friction activated.

Table 1 Measurements and SWAN results at various locations in the Haringvliet and Saginaw Bay of significant wave height H_s and mean wave period T_M .

Location	Measurements		SWAN results			
	H_s (m)	T_M (s)	"wind"		"no wind"	
			H_s (m)	T_M (s)	H_s (m)	T_M (s)
Haringvliet						
1	3.54	6.6	3.54	6.6	3.54	6.6
2	—	—	3.22	6.8	3.32	6.6
3	2.63	6.4	2.85	6.9	2.85	6.8
4	2.71	6.3	2.82	6.9	2.81	6.8
5	0.79	3.2	0.95	6.0	0.82	6.8
6	1.41	4.9	1.54	6.5	1.42	6.8
7	1.84	6.0	1.77	6.7	1.66	6.9
8	1.08	3.7	1.00	5.2	0.65	6.4
Saginaw Bay						
A	1.90	7.3	1.91*	7.3*	1.92*	7.3*
B	0.94	4.2	0.80	3.7	0.23	6.9
C	1.30	—	0.78	3.5	0.07	5.3

* fitted.

A comparison of the significant wave height between "wind" and "no wind" shows the relative importance of wind effects on the significant wave height deep inside in the branch (1.00 m versus 0.65 m at location 8). It is obvious that the added wind input, whitecapping and the quadruplet wave-wave interactions were essential to obtain the better results ("wind") deep inside the Haringvliet. The regeneration of waves is clearly visible as a second, high frequency peak in the spectrum (see Fig. 4). This secondary peak shifts the mean frequency to higher values but not sufficiently (compare the computed and observed mean wave period T_M in Table 1), most probably because the triad interactions are absent in the present version of SWAN.

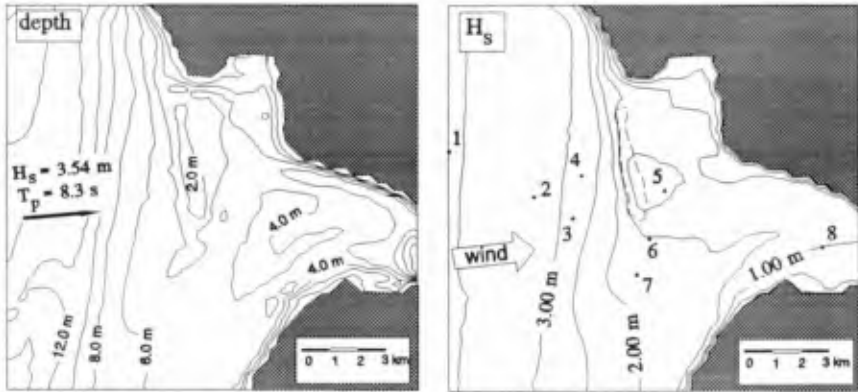


Fig. 2 Left-hand panel: the bathymetry of the Haringvliet area (contour line interval 2 m). Right-hand panel: results of the SWAN computation in terms of significant wave heights (all mechanisms activated) and location of the eight buoys. The dashed line indicates the location of the shoal.

Model results for Saginaw Bay

We carried out the calculations for Saginaw Bay using the same bottom grid resolution of 1200 m by 1200 m as used by Bondzie and Panchang (1993). To assume an up-wind boundary that is as homogeneous as possible, we choose this boundary at a line just outside the bay (the right-hand boundary of Fig. 3). Since the observations were taken during a storm, we assume a $\cos^2(\theta)$ distribution and a JONSWAP spectrum at this up-wave boundary. For such conditions, a directional resolution of $\Delta\theta=10^\circ$ is sufficient. We used a frequency resolution $\Delta f=0.1225 \cdot f$ between 0.555 Hz and 1. Hz. The significant wave height and peak period at the up-wave boundary was chosen such that at location A the model reproduces the observed wave height and period (Table 1). The calculated pattern of the significant wave height is shown in Fig. 3. The wave height gradually decreases between the up-wave boundary and the entrance of the bay. Due to depth effects, more wave energy penetrates into the deeper entrance than into the shallower entrance of the bay (roughly 20 % lower wave height near location A than in the other entrance). As the waves penetrate into the bay they refract laterally to the shallower parts of the bay. The calculated significant wave heights and mean periods at the three wave gauges are shown in Table 1. In contrast with the observations, the calculated wave height shows no growth between gauge B and C at all. Calculations with a 25% higher wind speed, which is fairly realistic since the wind speed was recorded on land, also did not show the observed growth (similarly for a 50% higher wind speed). Additional computations with another third-generation wave model

(WAVEWATCH; Tolman, 1991, 1992) also failed to reproduce the observed net growth. Also the HISWA model failed in this (Bondzie and Panchang, 1993; who used an uniform wave boundary condition along a straight line across the entrance through location A). Still the effect of wind on the significant wave height deep inside the bay is clearly visible in the model as shown in Table 1 (0.78 m versus 0.07 m at location C) and Fig. 4. Apparently the decay of the low-frequency part of the spectrum is compensated by the growth of the high-frequency part.

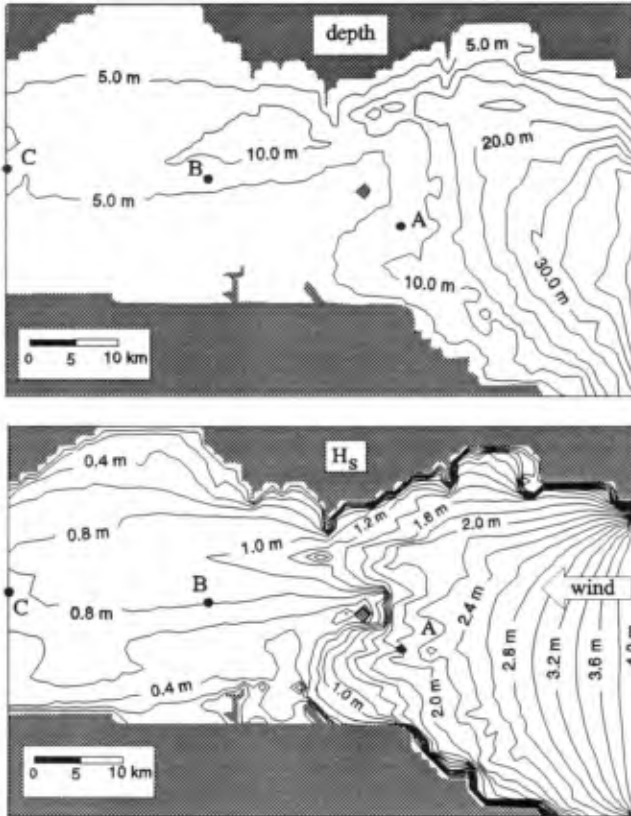


Fig. 3 Top panel: the bathymetry of Saginaw Bay (contour line interval 5 m). Bottom panel: results of the SWAN computation in terms of significant wave heights (all mechanisms activated) and the locations of the three wave gauges.

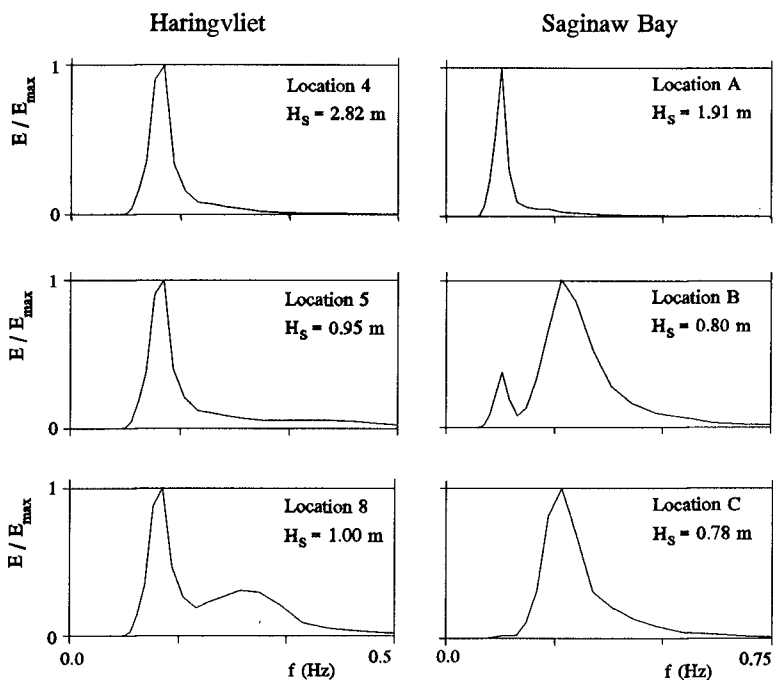


Fig. 4 Left-hand panels: Computed, normalized frequency spectra at location 4, 5 and 8 of the Haringvliet. Right-hand panels: Computed, normalized frequency spectra at locations A, B, and C of Saginaw Bay.

Conclusions and future work

We have described the second phase in the development of a third-generation fully spectral wave model for near-shore applications (SWAN) that is stationary and unconditionally stable. This permits economically feasible, high-resolution computations with all relevant effects of propagation, generation and dissipation included without a priori restraints on the development of the wave spectrum. The present version includes refractive propagation (currents included), wind generation, quadruplet wave-wave interactions, whitecapping, bottom friction, depth-induced breaking and wave blocking.

We have performed a number of computations with the SWAN model in two cases: the Haringvliet and Saginaw Bay. In the Haringvliet case the agreement of the computed significant wave heights with the observations is reasonable in spite of the absence of the triad interactions. We have found in Saginaw Bay a significant

difference between the calculated and observed wave heights deep inside the bay. Although the effect of regeneration of waves by wind is clearly visible in the model, we could not reproduce the observed wave growth between location B and C, even when we increased the wind speed. The wave periods are not properly computed, in particular in the Haringvliet case. This underscores the importance of the next phase in the development of the SWAN model in which a parameterized formulation for the triad wave-wave interactions will be implemented.

Acknowledgements

We thank our colleagues C. Bondzie and V.G. Panchang of the University of Maine for providing us with the data of Saginaw Bay. We also thank H.L. Tolman for his permission to use the WAVEWATCH II model for the Saginaw Bay computation.

References

- Abbott, M.B. and D.R. Basco (1989). *Computational Fluid Dynamics*, Jonh Wiley & Sons, Inc., New York, 425 p.
- Abreu, M., A. Larraza and E. Thornton (1993). Nonlinear transformation of directional spectra in shallow water. *J. Geophysical Res.*, 97 (C10), 15,579-15,589.
- Battjes, J.A. and J.P.F.M. Janssen (1978). Energy loss and set-up due to breaking of random waves. *Proc. 16th Int. Conf. Coastal Engineering*, Hamburg, 569-587.
- Battjes, J.A., Y. Eldeberky and Y. Won (1993). Spectral Boussinesq modelling of random, breaking waves. *Proc. of 2nd Int. Symposium on Ocean Wave Measurement and Analysis*, New Orleans, 813-820.
- Beji, S and J.A. Battjes (1993). Experimental investigation of wave propagation over a bar. *Coastal Engineering*, 19, 151 - 162.
- Bondzie, C. and V.G. Panchang (1993). Effect of bathymetric complexities and wind generation in a coastal wave propagation model. *Coastal Engineering*, 21, 333-366.
- Bouws, E. and G.J. Komen (1983). On the balance between growth and dissipation in an extreme depth-limited wind-sea in the southern North sea. *J. Phys. Oceanography*, 13, 9, 1653-1658.
- Cavaleri, L. and P. Malanotte-Rizzoli (1981). Wind wave prediction in shallow water: Theory and applications. *J. Geophys. Res.*, 86, No. C11, 10, 961-973.
- Hasselmann, K. (1962). On the non-linear energy transfer in a gravity wave spectrum. Part 1. General theory. *J. Fluid Mech.*, 12, 481-500.
- Hasselmann, K. (1963). On the non-linear energy transfer in a gravity wave spectrum. Part 2. Conservation theorems; wave-particle analogy; irreversibility. *J. Fluid Mech.*, 15, 273-281.

- Hasselmann, K., T.P. Barnett, E. Bouws, H. Carlson et al. (1973). Measurements of wind-wave growth and swell decay during the Joint North Sea Wave Project (JONSWAP). *Ergänzungsheft zur Deutschen Hydrographischen Zeitschrift*, 12.
- Hasselmann, K. (1974). On the spectral dissipation of ocean waves due to whitecapping. *Boundary-Layer Meteorology*, Vol. 6, No. 2, 200-228.
- Hasselmann, K. and S. Hasselmann (1985). Computations and parameterizations of the nonlinear energy transfer in a gravity-wave spectrum. Part I: A new method for efficient computations of the exact nonlinear transfer integral. *J. Phys. Oceanography.*, 15, 1369-1377.
- Holthuijsen, L.H., N. Booij and T.H.C. Herbers (1989). A prediction model for stationary, short crested waves in shallow water with ambient currents. *Coastal Engineering*, 13, 23 - 54.
- Holthuijsen, L.H., N. Booij and R.C. Ris (1993). A spectral wave model for the coastal zone. *Proc. of 2nd Int. Symposium on Ocean Wave Measurement and Analysis*, New Orleans, 630-641.
- Komen, G.J., S. Hasselmann and K. Hasselmann (1984). On the existence of a fully developed wind-sea spectrum. *J. Phys. Oceanography.*, 14, 1271-1285.
- Komen, G.J., L. Cavaleri, M. Donelan, K. Hasselmann, S. Hasselmann and P.A.E.M. Janssen (1994). *Dynamics and modelling of ocean waves*. Cambridge University Press, UK, 560 p.
- Madsen, P.A., R. Murray and O.R. Sørensen (1991). A new form of the Boussinesq equations with improved linear dispersion characteristics. *Coastal Engineering*, 15, 4, 371-388.
- Phillips, O.M. (1958). The equilibrium range in the spectrum of wind-generated waves. *J. Fluid Mech.*, 4, 426-434.
- Phillips, O.M. (1977). *The dynamics of the upper ocean*, 2nd edition, Cambridge University Press, 261 p.
- Snyder, R.L., F.W. Dobson, J.A. Elliott and R.B. Long (1981). Array measurements of atmospheric pressure fluctuations above surface gravity waves. *J. Fluid Mech.*, 102, 1-59.
- Tolman, H.L. (1991). A third-generation model for wind waves on slowly varying unsteady, and inhomogeneous depths and currents. *J. Phys. Oceanography.*, 21, no. 6, 782-797.
- Tolman, H.L. (1992). Effects of numerics on the physics in a third generation wind-wave model. *J. Phys. Oceanography.*, 22, no. 10, 1095-1111.
- WAMDI group (Hasselmann et al.), 1988, The WAM model - a third generation ocean wave prediction model, *J. Phys. Oceanography*, 18, 1775-1810.